Structural characterization of the hydrogen-covered C(100) surface by density functional theory calculations

J. A. Steckel,* G. Kresse, and J. Hafner
Institut für Materialphysik and Center for Computational Materials Science, Universität Wien, Sensengasse 8/12, A-1090 Wien, Austria
(Received 27 May 2002; published 3 October 2002)

We present the results of a density functional theory (generalized gradient approximation) study of the hydrogenated C(100) surfaces. We have analyzed the formation energy of phases with different hydrogen coverages ($\theta = 1.0$, 1.2, 1.33, 1.5, and 2.0) as a function of the hydrogen chemical potential. As the hydrogen chemical potential increases, the stable phase changes from the bare surface through all the hydrides considered, in order of increasing coverage. The value of the hydrogen chemical potential beyond which dihydride units are stabilized on the surface nearly coincides with the potential at which the the formation energy of methane is zero. However, since the desorption of hydrocarbons is an activated process, dihydride units can appear in metastable surface phases. To investigate this possibility, we have calculated vibrational frequencies for the (2×1):H, (5×1):1.2H, and (3×1):1.33H phases of the H/C(100) surface. The presence of a dihydride unit on the surface leads to a H-C-H bending mode with a frequency near 1475 cm^{-1}. Because there is no vibrational mode with a frequency in this region of the spectrum for the monohydride surface, this peak may be viewed as evidence that dihydride units are present on the surface.

DOI: 10.1103/PhysRevB.66.155406 PACS number(s): 68.35.Ja, 68.47.−b, 68.43.Bc

I. INTRODUCTION

A cut through bulk diamond along the (100) plane leaves each surface C atom with two dangling bonds. The resulting surface undergoes reconstruction to a (2×1) phase, consisting of parallel rows of C-C ''dimers.''[1–5] The lowering of the surface energy due to the creation of the C-C bond is partially offset by bond-length distortions and introduction of strain that extends downward several layers into the bulk. The reconstruction leaves one dangling bond per surface atom and, hence, the surface remains quite reactive. Interactions between the dangling bonds on the surface C atoms impart a partial π-bond character to the dimers.[6,7] The dimers on the C(100) surface are symmetric, as opposed to dimers on the Si(100) surface, which are believed to be tilted due to a Jahn-Teller-like distortion.[8–10]

Hydrogen plays an important role in determining the structures and properties of diamond surfaces. Dangling bonds on the diamond surface are normally saturated with hydrogen atoms.[11] Hydrogen is essential for the growth of diamond films via chemical vapor deposition (CVD). Atomic hydrogen in hydrogen-hydrocarbon gas mixtures is believed to abstract hydrogen from the hydrocarbons to form methyl (or other) radicals, which can be incorporated into the growing surface. Hydrogen is known to preferentially etch graphitic carbon, and it has been suggested that, by tying up dangling bonds on the surface, it preserves the sp^3 hybridization of carbon atoms at the surface.[12] It has recently been shown that anisotropic etching of undercoordinated carbon atoms on the growing C(100) surface by hydrogen plays a crucial role in the production of smooth, well-ordered diamond surfaces.[13]

For hydrogen coverages up to 1 ML, the dimer reconstruction and the (2×1) symmetry remain intact and each carbon is capped by one hydrogen atom.[14–16] On the monohydride surface there is a lengthening of the dimer C-C bond (with respect to the bare dimer) as it acquires a single-bond character.

For increasing hydrogen coverages, a fraction of the surface carbons must be bonded to two hydrogen atoms to form dihydride (methylene) units. When two dihydride units occupy neighboring sites on the surface, repulsion between the hydrogen atoms becomes a major destabilizing factor. While the Si(100):2H surface is stable, it is not certain that the ordered, fully saturated dihydride surface is stable for diamond.[17] The critical difference is that the shorter C-C bond length leads to steric hindrance between neighboring dihydride units on the surface. On the symmetric Si(100)-(1×1):2H surface, hydrogen atoms on neighboring dihydride units are separated by $\sim$1.5 Å. On the symmetric C(100)-(1×1):2H surface, even with the H-C-H angle of the dihydride unit reduced from the ideal 109.47° to $\sim$85°, the distance between hydrogen atoms on neighboring dihydrides is only $\sim$1.0 Å.

The clean and hydrogen-covered C(100) surfaces have been modeled theoretically by a variety of techniques for hydrogen coverages ranging from $\theta = 0$ to 2.0.[17–30] For hydrogen coverages up to 1 ML, theoretical studies are in close agreement with respect to geometry and energetics.[19,20,24–28] However there are discrepancies and gaps in the theoretical results for higher hydrogen coverages. One question that remains open is whether ordered phases containing relatively few dihydrides separated by monohydride units are stable on the C(100) surface. In such phases, with hydrogen coverages only slightly higher than $\theta = 1.0$, the dihydride units are not obliged to reside directly next to one another. This is one of the motivations for our current work.

Several groups have studied hydride surfaces of diamond using density functional theory (DFT) calculations in the local density approximation (LDA) but to date there have been no studies using the generalized gradient approximation (GGA). For bulk diamond, a certain tendency to overbinding

(inflated values for cohesive energy and bulk modulus, undersized lattice constant) is evident in the LDA.[31] As we will discuss below, we find that this overbinding is to some extent corrected in the GGA. LDA calculations were performed by Furthmüller, Hafner, and Kresse, who investigated the bare surface, (2×1):H, and a ''pseudo''-(1×1):1.5H reconstruction with alternate rows of C atoms bonded to one and two H atoms, respectively.[25,27] DFT calculations using the LDA were performed by Hong and Chou, who plotted the stability of the (2×1):H, (3×1)1.33H, and (1×1):2H (canted) surface phases as a function of hydrogen chemical potential.[28] In this study, we present the results of a GGA study of the hydrides of the C(100) surface. We have considered many of the phases studied previously, and we have included also several additional configurations to model hydrogen coverage slightly higher than one monolayer.

A number of researchers have explored possible relaxation schemes for the (1×1):2H dihydride surface.[3,17–20,24,25,27–29] Yang and D'Evelyn performed a molecular mechanics study for a variety of coverages and found that H-H repulsion in the dihydride surface may be partly relieved by twisting the dihydride units around an axis perpendicular to the surface.[18] Zhang *et al*. used *ab initio* molecular dynamic (MD) simulations to study the clean and hydrogen-covered C(100) surface and predicted the dihydride to be energetically unstable relative to H_2 desorption. Their simulated annealing calculations of the dihydride surface resulted in a structure with the dihydride units canted with respect to the surface normal.[19] Winn *et al*. found, using semiempirical tight-binding molecular dynamics (TBMD), two additional low-energy structures for the dihydride surface, the lean-to and the herringbone structures, in which the separations between surface dihydride units are maximized at the expense of distortions in the subsurface layers.[20] The ideal, symmetric, and canted C(100):2H surfaces are expected to yield (1×1) low energy electron diffraction (LEED) patterns while the herringbone and lean-to configurations have (2×1) symmetry.[14] In this study we have done a comparison of the symmetric, canted, twisted, lean-to, and herringbone phases of the (1×1):2H phase.

Vibrational frequencies of adsorbates have been calculated for the (2×1):H phase using empirical molecular mechanics MD simulations,[21] DFT (LDA),[28] TBMD,[29] and nonself-consistent Harris (LDA) methods.[26] In the TBMD study, the (1×1):2H phase was studied as well.[29] To date, no studies have reported calculated frequencies for coverages between $\theta=1.0$ and 2.0. In this study we present calculated vibrational frequencies for the (2×1):H, (3×1):1.33H, and (5×1):1.2H surfaces and a comparison is made with experimental results.

II. EXPERIMENTAL STUDIES

In experimental studies on diamond crystals using LEED and related methods, the as-polished C(100) surface was shown to undergo a transformation from a (1×1) to a (2×1) LEED pattern in a manner similar to the Si(100) surface but at higher temperatures, e.g., 1000 to 1200 K.[11,12,14,32–34] Hamza *et al.*[32] and Lee and Apai[11] reported that the reconstructed (2×1) surface could regain a (1×1) LEED pattern after atomic hydrogen dosing, but this result was not confirmed by either Thomas *et al.*[33] or Smentkowski *et al.*[14] It was shown that exposure of the C(100)-(2×1) surface to atomic oxygen restored the (1×1) LEED pattern, suggesting that an unreconstructed surface can be achieved if all dangling bonds are saturated.[33] Subsequently, advancements in growth techniques allowed researchers to grow much smoother diamond films and these films yielded exclusively a (2×1) LEED pattern.[35] Thoms *et al*. showed that hydrogen plasma treatment of synthetic diamonds produced smooth surfaces with large atomically flat domains that also exhibited only a (2×1) LEED pattern.[36,37] The same researchers showed that a synthetic diamond exhibited a (1×1) LEED pattern after acid treatment, but following the hydrogen plasma treatment, a (2×1) LEED pattern was obtained.[36] The (1×1) LEED pattern was attributed to the underlying diamond lattice of a disordered surface and the fact that it was so frequently observed was attributed to the *difficulty of producing smooth diamond surfaces*.[36,37] The nature of the disordered surface, including whether dihydride units are present, has not been fully elucidated.

Using LEED and high resolution electron energy loss spectroscopy (HREELS) Lee and Apai found evidence of carbon atoms bonded to multiple hydrogens on the C(100) surface of a polished natural diamond with a (1×1) LEED pattern.[11] In contrast, Aizawa *et al.* concluded that the (100) surface of a hydrogenated, CVD-grown diamond was terminated by monohydrides units.[35] A number of researchers in subsequent spectroscopy studies also concluded that the hydrogen-terminated C(100) surfaces on high-quality synthetic diamond surfaces are characterized by the monohydride species.[14,37]

In recent atomically resolved scanning tunneling microscopy (STM) studies of epitaxially grown C(100) surfaces, (2×1) dimer structures are dominant but local (3×1) reconstructions near step edges and on terraces are clearly observed as well as antiphase boundaries, pits, dimer vacancies, etc.[13,38,39] Stallcup and Perez have used ultrahigh vacuum, STM, and related techniques to show that the temperature of the surface during exposure to atomic hydrogen has a strong effect on the resulting morphology of the surface. Etching at 200 °C and 500 °C leads to rough and slightly smoother surfaces, respectively, while etching at 1000 °C leads to very smooth surfaces with (2×1) domains as large as 350 nm^2.[13] Lukins *et al.* have recently presented STM images, obtained in air, and interpreted to be the C(100)-(1×1):2H surface.[40] It is not clear, however, whether the diamond film in air after CVD growth is clean, or, as suggested by Stallcup and Perez, is covered with physisorbed hydrogen and carbon.[13]

III. METHODS

The DFT calculations were performed with the Vienna *ab initio* simulation package (VASP),[41,42] and made use of the projector augmented wave method of Blöchl and co-workers.[43,44] The plane-wave basis set included waves up to 400 eV. We used the Perdew and Zunger[45] parametrization of the local

exchange-correlation functional according to the quantum Monte Carlo simulations of Ceperley and Alder,[46] adding nonlocal corrections in the form of the GGA as presented by Perdew *et al.*[47] A comparison of values for the bulk modulus, equilibrium lattice constant, and cohesive energy shows that the GGA is at least as accurate as the LDA for the calculation of structural properties of bulk diamond, but provides a better description of the cohesive properties. The GGA (experimental, LDA) values for the bulk modulus and lattice constant are 4.24 (4.43, 4.60) Mbars and 3.574 (3.567, 3.528) Å, respectively.[48] While the tendency of the LDA method for overbinding leads to an overestimation of the bulk modulus and an underestimation of the lattice constant, the GGA method leads to a small tendency for underbinding in bulk diamond. The GGA value for the cohesive energy of -7.83 eV/atom is lower than the value of -9.00 eV/atom calculated using the LDA by Furthmüller *et al.*,[48] but when compared to the experimental value of 7.37 eV/atom, can be seen as a vast improvement over the LDA. We calculated the bulk optical phonons at the Γ point and our result of $\sim 1290\ \mathrm{cm}^{-1}$ shows a decrease from the LDA value of $\sim 1310\ \mathrm{cm}^{-1}$, while the experimental value is $1315s\ \mathrm{cm}^{-1}$.[31,49] The slight decrease of the phonon frequencies is evidently related to the lattice expansion induced by the GGA; we find, in agreement with other studies, that the effect of the GGA on vibrational properties is modest.[50]

For the discussions to follow, it will be useful to define the formation energy Ω per (1×1) unit cell, at zero temperature, and ignoring the zero-point energy, as

$$\Omega = (E - n_C\mu_C - n_H\mu_H)/(1\times1), \tag{1}$$

where E is the total internal energy calculated with density functional theory, n_C and n_H are the numbers of C and H atoms present in the model, μ_C and μ_H are the chemical potentials of carbon and hydrogen, respectively, and the quantity is divided by the number of (1×1) unit cells. Although zero-point energy associated with lightweight hydrogen atoms may be large, since it is the difference in the zero-point energies between various systems that is important, these may reasonably be neglected.[20] The chemical potential μ_C is set equal to its value in bulk diamond, assuming equilibrium between the free surface and the bulk. In the case of the bare surface, Eq. (1) takes the value of the surface energy per (1×1) unit cell.

Four supercells were considered: a (2×2) and a (4×1) supercell, both with four C atoms per layer, a (3×1) supercell with three C atoms per layer, and a (5×1) supercell with five C atoms per layer. (2×2) supercells with 10, 12, and 14 layers were considered; changing from 10 to 12 layers changes the surface energy for the bare, ideal (1×1) by only 1.6 meV/(1×1) unit cell, and changing from 12 to 14 layers changes the same quantity by less than 0.4 meV/(1×1) unit cell. Therefore, models with 12 layers of carbon atoms were used. A vacuum layer of eight layers was introduced to separate the the slabs. During relaxations, the four bottom most carbon layers were kept fixed at bulk positions. Saturation of the bottom most layer of C atoms in the slab by hydrogen atoms was found to have a negligible effect on the energetics and virtually no effect on the geometry; the production calculations, therefore, were carried out without hydrogen saturation.

Brillouin-zone integrations were performed on a grid of $4\times4\times1$ $(3\times8\times1,\ 2\times8\times1,\ 2\times8\times1)$ k points for the (2×2) [(3×1), (4×1), and (5×1)] supercells, respectively. For the (2×2) supercell, calculations were performed also on a series of grids up to a $6\times6\times1$ grid to verify that the energies are converged with respect to k-point sampling. On increasing from the $4\times4\times1$ to the $6\times6\times1$ grid, the total energies change by less than 10 meV. To determine the partial occupancies for each wave function, the Gaussian smearing method was adopted with a width of 0.05 eV. Minimum-energy structures were obtained by minimization of the forces according to a quasi-Newton (variable metric) algorithm.[51]

For $\theta = 1.0$, 1.2, and 1.33, harmonic vibrational frequencies for the top layer of carbon atoms and the hydrogen atoms were computed by diagonalizing the mass-weighted second-derivative (dynamical) matrix. The general scheme followed to construct the dynamical matrix was to displace each atom from its equilibrium position and to calculate the forces acting on all the atoms in each direction.[31] The second derivative of the Hamiltonian was estimated from the forces according to the finite difference approach. In our calculations, we used four displacements per atom, each of 0.04 Å, to estimate the second derivatives. In each of the three supercells, the atoms displaced consisted of the top layer of C atoms as well as all of the H atoms, while all other atoms were held fixed. As a control, we calculated the frequencies for the (3×1):1.33H phase, allowing movement of all the hydrogen atoms plus the three uppermost layers of C atoms; the resulting vibrational frequencies differ by less than 3% from the calculations in which only the hydrogen atoms and uppermost layer of C atoms were moved. The intensities of the loss peaks associated with each normal mode were calculated based on an estimation of the derivative of the dipole with respect to the atomic positions (the dynamical dipole). For the frequency calculations, the (2×1):H surface was modeled using a (4×1) supercell.

IV. STRUCTURE AND STABILITY OF HYDROGENATED C(100) SURFACES

The structures studied include (a) the bare reconstructed (2×1) C(100) surface, (b) the (2×1):H monohydride surface, (c) the (5×1):1.2H surface, consisting of two monohydride dimer units alternating with one dihydride unit, (d) the (3×1):1.33H surface, with alternating monohydride and dihydride units, (e) the (4×1):1.5H surface, consisting of one monohydride unit alternating with two dihydride units, and (f) the (1×1):2H dihydride surface. Top and side views of these structures are presented in Fig. 1 and a comparison of the geometric parameters with previous results is presented in Table I.

The bare C(100) surface was modeled with a (2×2) supercell with four C atoms per layer. The clean surface with the ideal geometry of the bulk has a calculated surface energy of 3.48 eV per (1×1) unit cell [defined according to

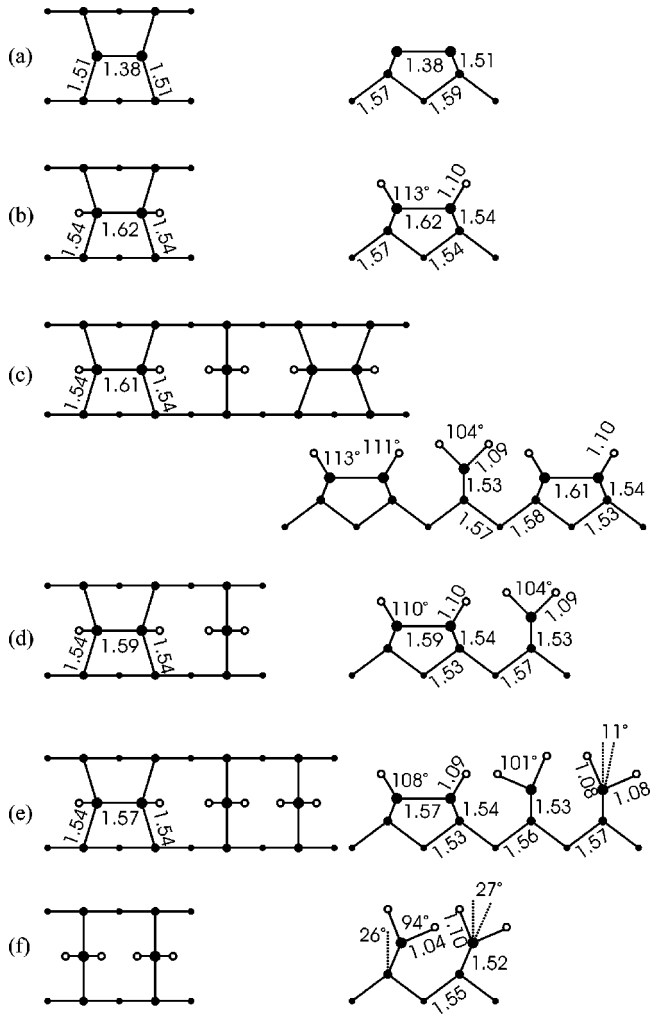

FIG. 1. Top and side views of the C(100) surface: (a) bare (2×1) dimer surface, (b) monohydride (2×1):H, (c) monohydride-dihydride-monohydride (5×1):1.2H, (d) monohydride-dihydride (3×1):1.33H, (e) monohydride-dihydride-dihydride (4×1):1.5H, (f) dihydride (canted configuration) (1×1):2H. Filled circles represent carbon atoms; open circles represent hydrogen atoms. Bond lengths are marked along connecting lines (in angstroms), and selected angles are labeled.

Eq. (1)], which is significantly lower than the LDA value of 3.89 eV per (1×1) unit cell.[25] Relaxation of the (1×1) surface structure lowers the energy by −0.12 eV/(1×1) unit cell. The reconstruction to the (2×1) dimer structure lowers the energy by an additional −1.46 eV/(1×1) unit cell. This is only slightly lower than the energy gain due to reconstruction calculated in the LDA [−1.51 eV/(1×1) unit cell].[25] The calculated dimer length of 1.38 Å is in close agreement with the LDA results of Furthmüller *et al.*,[25] Hong and Chou,[28] and Zhang *et al.*[19] The TBMD calculations of Winn *et al.* on the other hand, lead to a longer C-C bond length.[20]

In the (2×1):H monohydride, it can be seen that the saturation of the surface C atoms by hydrogen changes the character of the C-C surface dimer from π to σ; its length increases to 1.62 Å. The GGA causes an increase of the bond length by only 0.01 Å compared to the LDA result. Our calculated structure is in good agreement with the structural parameters for this surface recently reported in the LEED study by Wang *et al.*[15]

As hydrogen coverage increases beyond 1 ML, surface dihydride units are introduced. In general, the C-H bond in a dihydride is only slightly shorter than the C-H bond in a monohydride unit, but the C-C-H angles are reduced more noticeably. The introduction of one dihydride unit between two monohydrides causes little or no change in the structure of neighboring monohydride units, but as the number of dihydride units increases, some contraction in the structural parameters of the neighboring monohydride units is evident and the structural parameters of the dihydride units also show evidence of steric repulsion. We modeled the $\theta=1.2$ surface using a (5×1) supercell. In our calculated structure, each dihydride is separated by two monohydride units. Virtually the only change in the structure of the monohydride units, compared to the $\theta=1.0$ surface, is a shortening of the dimer bond from 1.62 to 1.61 Å. The $\theta=1.33$ surface was modeled with a (3×1) supercell and it was found that the increase in the ratio of dihydride to monohydride units causes the dimer C-C bond to shorten to 1.59 Å. In addition, there is a decrease in the H-C-C angles of the monohydride units from 113° to 110°.

In the (4×1):1.5H model, as the ratio of dihydride to monohydride units increases further, the same trends continue with the dimer bond length becoming 1.57 Å and the H-C-C angle of the monohydride unit decreasing again to 108°. The structural parameters of the dihydride units themselves also indicate increased H-H repulsion on the surface, as the H-C-H bond of the dihydride decreases from 104° on the $\theta=1.2$ and $\theta=1.33$ surfaces to 101° on the $\theta=1.5$ surface. Some reduction of the steric hindrance on the $\theta=1.5$ surface is gained by a canting of the dihydride units, with each dihydride canting by about 11° away from the symmetric position (see Fig. 1).

We have examined five previously proposed configurations for the $\theta=2.0$ surface using a (2×2) supercell. The symmetric dihydride structure yields a formation energy of $\Omega=-5.37$ eV/(1×1) unit cell [as defined in Eq. (1)]. For the twisted configuration, we find a formation energy of $\Omega=-5.38$ eV/(1×1) unit cell and a twisting angle of only 8°, which is significantly smaller than the angles found in previous studies. For example, the twisting angle reported by Winn *et al.* was 33° and that reported by Hong and Chou was 19°.[20,28] The formation energies of the herringbone surface and lean-to surfaces are $\Omega=-5.47$ and −5.54 eV/(1×1) unit cell, respectively, while that for the canted surface was $\Omega=-5.71$ eV/(1×1) unit cell. Therefore the canted configuration is the most stable structure found for the C(100):2H surface. The relative stabilities of the five dihydride configurations are directly related to the minimum distances between H atoms on neighboring dihydride units on the surfaces. The symmetric surface places H atoms within 1.10 Å of one another, the twisted surface relaxes the distance to 1.13 Å, the herringbone and lean-to surfaces increase the distance to 1.24 and 1.27 Å, respectively, and the

TABLE I. Comparison of geometrical parameters for H/C(100) with previous work. The d(H-H) parameter refers to the distance between the two nearest-neighbor H atoms on the surface. Distances are given in angstroms.

		Present work	Ref. 25[a]	Ref. 28[b]	Ref. 15[c]
(2×1)	d_{11}(C-C) dimer	1.38	1.37	1.37	
	d_{12}(C-C)	1.51	1.50	1.50	
(2×1):H	d(C-H)	1.10	1.10	1.11	
	d_{11}(C-C) dimer	1.62	1.61	1.63	1.60
	d_{12}(C-C)	1.54	1.53	1.53	1.57
	∠H-C-C	113°		113°	
	d(H-H)	2.55			
(5×1):1.2H	d(C-H) monohydride	1.10			
	d_{11}(C-C) dimer	1.61			
	d_{12}(C-C) monohydride	1.54			
	∠H-C-C monohydride	113°			
	d(C-H) dihydride	1.09			
	d_{12}(C-C) dihydride	1.53			
	∠H-C-H dihydride	104°			
	d(H-H)	1.80			
(3×1):1.33H	d(C-H) monohydride	1.10		1.10	
	d_{11}(C-C) dimer	1.59		1.58	
	d_{12}(C-C) monohydride	1.54		1.53	
	∠H-C-C monohydride	110°		110°	
	d(C-H) dihydride	1.09		1.10	
	d_{12}(C-C) dihydride	1.53		1.51	
	∠H-C-H dihydride	104°		103°	
	d(H-H)	1.76			
(4×1):1.5H	d(C-H) monohydride	1.09			
	d_{11}(C-C) dimer	1.57			
	d_{12}(C-C) monohydride	1.54			
	∠H-C-C monohydride	108°			
	d(C-H) dihydride	1.08			
	d_{12}(C-C) dihydride	1.53			
	∠H-C-H dihydride	101°			
	d(H-H)	1.37			
(1×1):2H	d(C-H)	1.10, 1.04		1.11,1.05	
	d_{12}(C-C)	1.52		1.51	
	∠H-C-H	94°		91°	
	d(H-H)	1.36			

[a]Furthmüller *et al.*, LDA.
[b]Hong and Chou, LDA.
[c]Wang *et al.*, LEED.

canted structure places H atoms at a distance of 1.36 Å to one another.

In order to compare the stability of phases with differing amounts of hydrogen coverage, it is helpful to compare their formation energies [according to Eq. (1)] as a function of the H chemical potential.[20,28,52] The calculated formation energies per (1×1) unit cell are shown in Fig. 2 as a function of hydrogen chemical potential. The chemical potential is measured relative to the calculated energy of the H_2 molecule, e.g.,

$$\mu_H = \frac{1}{2}E(H_2). \quad (2)$$

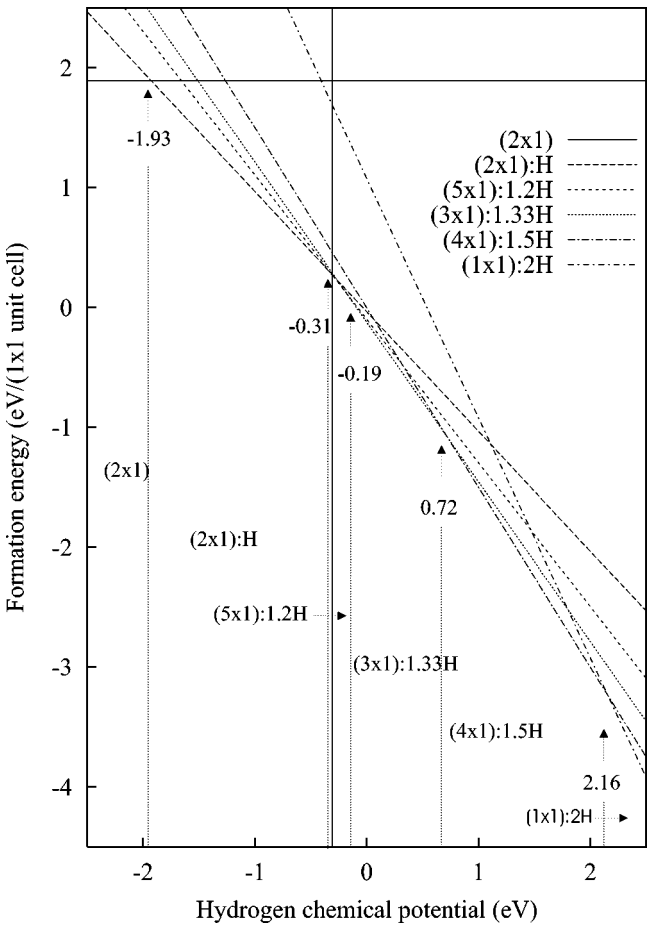

FIG. 2. Formation energy Ω [in eV per (1×1) unit cell] of hydrides of the C(100) surface as a function of hydrogen chemical potential, μ_H (in eV). The horizontal line at $\Omega=1.89$ eV per (1×1) unit cell corresponds to the formation energy of the bare (2×1) surface. As μ_H increases, the (2×1) bare surface, (2×1):H, (5×1):1.2H, (3×1):1.33H, (4×1):1.5H, and (1×1):2H phases successively become the most stable. The phases boundaries, marked by arrows, are at $\mu_H=-1.93$, -0.31, -0.19, 0.72, and 2.16 eV. The vertical line at $\mu_H=-0.309$ eV denotes the chemical potential at which the formation energy for CH_4 is zero.

The range of stability for the different surface hydrides varies with the hydrogen potential. Below $\mu_H=-1.93$ eV the bare reconstructed (2×1) surface is most stable. The C(100)-(2×1):H surface is stable over a large portion of the range of hydrogen chemical potential. As the hydrogen chemical potential increases to $\mu_H=-0.31$ eV, the introduction of dihydride units becomes more favorable and the (5×1):1.2H phase becomes the most stable for a very short range of chemical potential. At $\mu_H=-0.19$ eV, the (3×1):1.33H phase becomes the most stable. At $\mu_H=0.72$ eV, the (4×1):1.5H phase becomes most stable and at $\mu_H=2.16$ eV, the (1×1):2H is finally the most stable. Following Hong and Chou,[28] we have added to Fig. 2 a vertical line to mark the calculated value of the hydrogen chemical potential at which CH_4 forms at no energy cost ($\mu_H=-0.309$ eV). On the right-hand side of the vertical line, the formation energy of CH_4 is negative and therefore it should be considered a competing process. However, as desorption of CH_4 from the hydrogenated surface is an activated process, it is still possible that higher H coverages are found experimentally (as metastable states). For example, the range of hydrogen chemical potential where the (3×1):1.33H phase is most stable lies completely to the right of the vertical line in Fig. 2, yet this phase has been observed experimentally.[13]

To gain further insight into the stability of dihydride species on the various surface phases considered, it is useful to compare the adsorption energy per hydrogen relative to the monohydride surface,

$$\Delta E_{ads}=\frac{1}{n_H}[E_{hydride}-E_{(2\times1):H}-n_H\tfrac{1}{2}E(H_2)], \qquad (3)$$

where $E_{hydride}$ is the energy of the hydride surface, $E_{(2\times1):H}$ is the energy of the (2×1):H monohydride surface, and $E(H_2)$ is the calculated energy of the H_2 molecule. For the (5×1):1.2H and (3×1):1.33H surfaces, the adsorption energies per hydrogen are -0.35 and -0.28 eV, respectively. For both of these phases the dihydride units are separated by monohydride units and the formation of the dihydride unit is an exothermic process. For the (4×1):1.5H surface, the adsorption energy is 0.06 eV. The destabilization caused by placing two dihydride units next to one another is clearly evident and the adsorption process is now slightly endothermic. This trend continues with the fully saturated (1×1):2H phases, where the energy of adsorption is positive for all of the configurations considered; the most favorable case, the canted configuration, yields a value of 1.1 eV.

Finally, we also consider the effect of the zero-point energy. To this end, we calculated the vibrational spectra (see also the following section) of three surfaces [(2×1):H, (5×1):1.2:H, and (3×1):1.33:H], and estimate the zero-point vibrational energy per hydrogen atom as

$$E_{\mathrm{ZPE}}=\frac{\hbar}{n_H}\sum_i \upsilon_i w_i, \qquad (4)$$

where the index i runs over all eigenmodes, υ_i is the corresponding vibrational frequency, and w_i is a weighting factor determined by the total norm of each eigenmode at the hydrogen atoms. Alternatively, we kept the substrate fixed and calculated the zero-point energy by summation over the vibrational modes. The calculated energies E_{ZPE} fall into the range of 312 to 326 meV per hydrogen atom for all the cases considered. This provides further support for the approximation made by Northrup[52] and Hong and Chou[28] that the zero-point energy of hydrogenated silicon and diamond surfaces may be reasonably approximated by a linear function of the number of hydrogen atoms in the unit cell.

We calculate the zero-point vibrational energy of the H_2 molecule to be 133 meV. Including these effects in the phase diagram in Fig. 2 shifts all curves $\approx$190 eV (320–130 meV) to the right. Therefore, while the inclusion of zero-point energy serves to make hydrogen adsorption on the surface slightly less favorable, it does not materially change the results presented above.

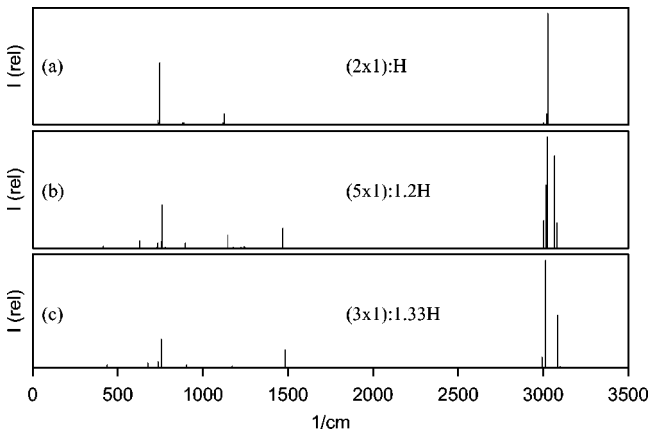

FIG. 3. Intensities of calculated vibrational frequencies for hydride phases of C(100): (a) monohydride (2×1):H, (b) (5×1):1.2H, (c) monohydride-dihydride (3×1):1.33H.

V. VIBRATIONAL SPECTROSCOPY OF HYDROGENATED SURFACES

Our calculations indicate that there is a high energy cost for placing two dihydride units next to one another. However, the cost for placing dihydride units between monohydride units, as in the (5×1):1.2H and the (3×1):1.33 hydride surfaces, is comparatively lower. In order to explore the possibility that dihydride units are present on slightly disordered diamond surfaces, we have calculated the vibrational modes of these hydride phases and compared them to experimentally measured spectra.

In Fig. 3 and Table II, we present calculated frequencies for the (2×1):H monohydride, the (5×1):1.2H, and the (3×1):1.33H hydride surfaces. We have set the intensities in Fig. 3 in proportion to the square of the calculated dynamic dipole moments. Certain modes should, by symmetry, have zero intensity, but in our calculations have small, finite intensities; this is caused by the numerical noise present in the calculations. For the C-C-H bending and the H-C-C-H stretching modes, comparison with the earlier MD simulations[21,29] and with experiment is complicated by the fact that all modes with frequencies lower than the zone-center optical modes couple to some degree with the bulk phonons.

The calculated spectrum of the (2×1):H surface, presented in Fig. 3(a), exhibits C-H symmetric and antisymmetric stretch peaks in the region of 3020 cm^{-1}. This C-H stretching frequency is higher than the frequencies calculated by Alfonso *et al.*[26] using the non-self-consistent Harris functional (2713–2750 cm^{-1}) and Smirnov and Raşeev using TBMD (2880–2934 cm^{-1}).[29] The overestimation with respect to the measured frequency of 2915 cm^{-1} obtained by Thoms and Butler is approximately 4%.[37] It is likely that anharmonic effects contribute to this discrepancy.[28] We find calculated H-C-C bending frequencies in the region of 1220 cm^{-1}. Aizawa *et al.* observed a band from 1000 to 1450 cm^{-1} with a clear peak visible at 1105 cm^{-1} in their HREELS study of synthetic diamond surfaces exhibiting a sharp (2×1) LEED pattern.[35] In the HREELS studies of Thoms and Butler, where a smooth, ordered (100) diamond surface was obtained by exposure to H plasma and where clear (2×1) LEED patterns were observed, the C-C-H bending peak was observed at 1250 cm^{-1}.[37,53] In our calculated spectrum, an intense mode is observed near 750 cm^{-1}; the normal mode associated with this loss is an in-phase ''bouncing'' motion of the H-C-C-H dimers. Given its low frequency, it is likely to couple to bulk phonons and, therefore, not be observed experimentally.

It can be seen from the calculated vibrational frequency spectra of the (3×1):1.33H surface [Fig. 3(b)] that the insertion of a dihydride unit leads to several clear changes. Symmetric and antisymmetric C-H stretching peaks appear for the dihydride unit near 3070 cm^{-1}. The symmetric C-H stretching peak for the monohydride unit appears at 3024 cm^{-1}. The H-C-H bending mode for the dihydride unit is predicted to have a frequency of 1469 cm^{-1}. Because there are no calculated frequencies in this region of the spectrum for the (2×1):H monohydride surface, this peak may be viewed as a signature for the presence of dihydride units. Indeed this peak is not seen in the recent HREELS studies of well-ordered, synthetic diamond surfaces, but in the earlier study of Lee and Apai of polished natural diamond, a peak at 1460 cm^{-1} was reported.[11] The authors noted that the sample exhibited a (1×1) LEED pattern. In the work of Smentkowski *et al.*[14] in which a natural, polished, single diamond crystal was used, a peak at $\sim$1480 cm^{-1} was partially obscured by a broad peak centered on 1210 cm^{-1}. A comparison of the HREELS spectra of Thoms and Butler with those of Lee and Apai reveals that the C-H stretching peak is narrow and centered on 2915 cm^{-1} in the former, while in the latter study it is broad and the authors have deconvoluted it into four peaks centered on 3070, 3010, 2915, and 2820 cm^{-1}. The authors attributed these peaks to the C-H stretching of sp^2 and sp^3 hybridized carbon, but we suggest an alternative interpretation: there could have been a significant amount of dihydride units on the (1×1) as-polished diamond surface.

Inspection of the calculated spectra of the (5×1):1.2H surface [Fig. 3(c)] reveals strong similarities to the (3×1):1.33H surface. An antisymmetric C-H stretch peak appears for the dihydride unit at 3086 cm^{-1}. The symmetric C-H stretch peak for the monohydride unit appears at 3014 cm^{-1}. The H-C-H bending mode for the dihydride unit is predicted to have a frequency of 1482 cm^{-1}.

VI. DISCUSSION

In this study, we present the results of a GGA study of the hydrides of the C(100) surface. We have modeled hydrogen coverages of $\theta=0$, 1.0, 1.2, 1.33, 1.5, and 2.0. Our predicted structure for the monohydride surface is in good agreement with the structural parameters reported in the LEED study by Wang *et al.*[15] For coverages only slightly higher than 1 ML, we find that the introduction of a dihydride unit produces little structural change in nearby monohydride units. As hydrogen coverage increases and the ratio of dihydride units to monohydride units increases, however, the steric repulsion

TABLE II. Calculated vibrational frequencies (ν, cm^{-1}) and intensities (I, arbitrary units) for hydride phases of C(100). Selected modes are identified. Abbreviations are sym. for symmetric, str. for stretch, ant. for antisymmetric, dihyd. for dihydride, and o.o.ph. for out of phase.

(2×1):H			$(5\times1)1.2$:H			$(3\times1)1.33$:H		
ν	I	Mode	ν	I	Mode	ν	I	Mode
3028	1.00	Sym. C-H str.	3082	0.23	Ant. dihyd. C-H str.	3100	0.02	Sym. dihyd. C-H str.
3019	0.10	Ant. C-H str.	3068	0.83	Sym. dihyd. C-H str.	3086	0.49	Ant. dihyd. C-H str.
3011	0.00	Sym. C-H str. (o.o.ph.)	3024	1.00	Sym. C-H str.	3014	1.00	Sym. C-H str.
3003	0.02	Ant. C-H str. (o.o.ph.)	3016	0.57	Sym. C-H str. (o. o. ph.)	2992	0.10	Ant. C-H str.
			3002	0.25	Ant. C-H str.			
			2992	0.00	Ant. C-H str. (o.o.ph.)			
			1469	0.18	H-C-H (dihyd.) bend	1482	0.17	H-C-H (dihyd.) bend
1221	0.00	H-C-C bend (o.o.ph.)	1245	0.01	H-C-C bend (o.o.ph.)	1280	0.01	H-C-C bend
1211	0.00	H-C-C bend	1243	0.02	H-C-C bend	1229	0.00	
1188	0.00		1225	0.01		1193	0.01	
1187	0.01		1197	0.00		1186	0.01	C-C (dimer) str.
1172	0.01		1193	0.00		1172	0.02	
1170	0.01		1177	0.01		1133	0.01	
1127	0.10	C-C (dimer) str.	1173	0.00				
1117	0.02		1147	0.12	C-C (dimer) str.			
			1140	0.00				
			1128	0.00				
889	0.02		897	0.05		943	0.01	
887	0.00		897	0.02		904	0.03	
882	0.02		896	0.00		892	0.00	
881	0.00		892	0.00		876	0.00	
862	0.01		887	0.00		791	0.00	
854	0.00		879	0.00		757	0.27	Dimer bounce
747	0.56	Dimer bounce	879	0.00		738	0.06	
740	0.02		779	0.01		725	0.00	
738	0.00		760	0.39	Dimer bounce	677	0.05	
737	0.04		758	0.06		439	0.03	
615	0.00		735	0.05				
599	0.00		732	0.01				
			721	0.00				
			630	0.00				
			629	0.07				
			416	0.02				

between H atoms on the surface becomes a serious destabilizing factor. The relative energies of the five fully hydrogen-saturated dihydride configurations considered are directly related to the H-H distances on the surface (with a larger H-H distance leading to a lower energy). We find the canted configuration to be lower in energy than the symmetric, twisted, herringbone, or lean-to configuration. This is in agreement with the LDA results of Hong and Chou[28] but in contradiction with the tight-binding MD simulations of Winn *et al.*[20] The disagreement between the tight-binding and *ab initio* results is related to the tendency of the former to underestimate the C-C bond strengths. The underestimation of the C-C bond length in the semiempirical model used in the tight-binding study lowers the energies of the herringbone and lean-to structures relative to the canted structure, because the herringbone and lean-to structures involve more distortion in the substrate than does the canted structure.

In order to compare the stability of phases with different hydrogen coverages, we have analyzed the formation energy as a function of the hydrogen chemical potential. As the hydrogen chemical potential increases, the stable phase is first the bare surface, then the monohydride, the (5×1):1.2H, the (3×1):1.33H, the (4×1):1.5H, and finally the (1×1):2H canted dihydride. The competing process of CH_4 formation is calculated to occur with no energy cost at a value of the hydrogen chemical potential within the range where the (5

×1):1.2H phase is most stable. However, the desorption of methane is an activated process, and would involve not just the formation of the methane molecule but substantial rearrangements of the C-C and C-H bonds of the surface. Therefore, this does not preclude the existence of metastable states consisting of mixed monohydride and dihydride units. The formation of relatively few dihydride units along with a preponderance of monohydride units could be favored at sufficiently high partial H pressures, even if the desorption of hydrocarbons occurs as a competitive process.

We have calculated vibrational frequencies for the (2×1):H, (5×1):1.2H, and (3×1):1.33H phases of the H/C(100) surface. For the (2×1):H surface, our calculated frequencies are in good agreement with recent experimental results using high-quality synthetic diamonds that exhibit a clear (2×1) LEED pattern. The insertion of a dihydride unit to the surface phase leads to several changes in the calculated spectra, the most obvious being a H-C-H bending mode with a frequency near 1480 cm^{-1}. Lee and Apai reported a peak at 1460 cm^{-1} in their 1993 study of polished natural diamond;[11] a peak in this frequency range has also been reported in another study of natural diamond surfaces.[14] In both studies, (1×1) LEED patterns were reported. Because there is no vibrational mode with a frequency in this region of the spectrum for the monohydride surface, this peak may indicate that the natural, polished diamond surfaces used in the earlier studies of H/C(100) contained significant numbers of dihydride units. It is possible to conceive of a surface that does not exhibit long-range order, is punctuated by step edges and pits, and consists of local domains of (2×1) as well as small domains of higher coverage such as (5×1):1.2H and (3×1):1.33H.

VII. CONCLUSIONS

We have used *ab initio* density functional theory in the form of the generalized gradient approximation to investigate the structural, vibrational, and thermodynamic properties of hydrogenated C(100) surfaces. For the clean and monohydride surfaces, the structural data are in good agreement with earlier studies performed in the local density approximation[19,25,27,28] and with experiment.[15] We have performed an analysis of the energy of formation of various surface phases as a function of the hydrogen chemical potential (corresponding to the hydrogen partial pressure above the surface). As hydrogen chemical potential increases, dihydride units appear in addition to monohydride dimers, and the most stable phase progresses from the bare surface through the (2×1):H, the (5×1):1.2H, (3×1):1.33H, (4×1):1.5H, and finally to the (1×1):2H dihydride surface. However, dihydride units are stabilized only at values of the hydrogen chemical potential where the formation of methane (i.e., etching) becomes thermodynamically favorable. Nevertheless, because the formation of methane at the surface necessitates surmounting an energy barrier, domains with dihydride units are possible on the H/C(100) surface; this is in agreement with recent STM observations.[13] Calculation of the vibrational properties demonstrates that infrared intensities observed near 1480 cm^{-1} arise from H-C-H bending modes and represent a clear signature for the presence of dihydride units on the surface.

Note added in proof. Recently, we became aware of a density functional theory study by S. Hong, Phys. Rev. B **65**, 153408 (2002), in which several structures for the dihydride surface of the C(100) surface are compared, and in which the energy ordering and conclusions regarding the dihydride phase are in agreement with those presented in this paper.

ACKNOWLEDGMENTS

This work was supported by the Austrian Science Funds within the Joint Research Project ''Gas-Surface Interactions'' (S8106-PHYS).

*Email address: jan.steckel@univie.ac.at

[1] T. Tsuno, T. Imai, Y. Nishivayashi, K. Hamada, and F. Fujimori, Jpn. J. Appl. Phys., Part 1 **30**, 1063 (1991).
[2] H.-G. Busmann, W. Zimmermann-Edling, H. Sprang, H.-J. Güntherodt, and I.V. Hertl, Diamond Relat. Mater. **1**, 979 (1993).
[3] T. Frauenheim, U. Stephan, P. Blaudeck, D. Porezag, H.-G. Busmann, W. Zimmermann-Edling, and S. Lauer, Phys. Rev. B **48**, 18 189 (1993).
[4] C. Yang and H. Kang, Phys. Rev. B **110**, 11 029 (1999).
[5] B. Weiner, S. Skokov, and M. Frenklach, J. Chem. Phys. **102**, 5486 (1995).
[6] T.L. Hukka, T.A. Pakkanen, and M.P. D'Evelyn, J. Phys. Chem. **98**, 12 420 (1994).
[7] D.R. Fitzgerald and D.J. Doren, J. Am. Chem. Soc. **122**, 12 334 (2000).
[8] J.E. Northrup, Phys. Rev. B **47**, 10 032 (1993).
[9] C. Kress, M. Fiedler, W.G. Schmidt, and F. Bechstedt, Phys. Rev. B **50**, 17 697 (1994).
[10] P. Krüger and J. Pollmann, Phys. Rev. Lett. **74**, 1155 (1995).
[11] S.-T. Lee and G. Apai, Phys. Rev. B **48**, 2684 (1993).
[12] P.G. Lurie and J.M. Wilson, Surf. Sci. **65**, 453 (1977).
[13] R.E. Stallcup II and J.M. Perez, Phys. Rev. Lett. **86**, 3368 (2001).
[14] V.S. Smentkowski, H. Jänsch, M.A. Henderson, and J.T. Yates, Jr., Surf. Sci. **330**, 207 (1995).
[15] Y.M. Wang, K.W. Wong, S.T. Lee, M. Nishitani-Gamo, I. Sakaguchi, K.P. Loh, and T. Ando, Phys. Rev. B **59**, 10 347 (1999).
[16] Y.M. Wang, K.W. Wong, S.T. Lee, M. Nishitani-Gamo, I. Sakaguchi, K.P. Loh, and T. Ando, Diamond Relat. Mater. **9**, 1582 (2000).
[17] S.H. Yang, D.A. Drabold, and J.B. Adams, Phys. Rev. B **48**, 5261 (1993).
[18] Y.L. Yang and M.P. D'Evelyn, J. Am. Chem. Soc. **114**, 2796 (1992).
[19] Z. Zhang, M. Wensell, and J. Bernholc, Phys. Rev. B **51**, 5291 (1995).
[20] M.D. Winn, M. Rassinger, and J. Hafner, Phys. Rev. B **55**, 5364 (1997).
[21] L. Zhigilei, D. Srivastava, and B.J. Garrison, Surf. Sci. **374**, 333 (1997).
[22] S.P. Mehandru and A.B. Anderson, Surf. Sci. **248**, 36 (1991).

[23] X.M. Zheng and P.V. Smith, Surf. Sci. **256**, 1 (1991).
[24] B.N. Davidson and W.E. Pickett, Phys. Rev. B **49**, 11 253 (1994).
[25] J. Furthmüller, J. Hafner, and G. Kresse, Europhys. Lett. **28**, 659 (1994).
[26] D.R. Alfonso, D.A. Drabold, and S.E. Ulloa, Phys. Rev. B **51**, 1989 (1995).
[27] J. Furthmüller, J. Hafner, and G. Kresse, Phys. Rev. B **53**, 7334 (1996).
[28] S. Hong and M.Y. Chou, Phys. Rev. B **55**, 9975 (1997).
[29] K.S. Smirnov and G. Raşeev, Surf. Sci. **459**, 124 (2000).
[30] H. Tamura, H. Zhou, K. Sugisako, Y. Yokoi, S. Takami, M. Kubo, K. Teraishi, A. Miyamoto, A. Imamura, M.N. Gamo, and T. Ando, Phys. Rev. B **61**, 11 025 (2000).
[31] G. Kresse, J. Furthmüller, and J. Hafner, Europhys. Lett. **32**, 729 (1995).
[32] A.V. Hamza, G.D. Kubiak, and R.H. Stulen, Surf. Sci. **237**, 35 (1990).
[33] R.E. Thomas, R.A. Rudder, and R.J. Markunas, J. Vac. Sci. Technol. A **10**, 2451 (1992).
[34] B.B. Pate, Surf. Sci. **165**, 83 (1986).
[35] T. Aizawa, T. Ando, M. Kamo, and Y. Sato, Phys. Rev. B **48**, 18 348 (1993).
[36] B.D. Thoms, M.S. Owens, J.E. Butler, and C. Spiro, Appl. Phys. Lett. **65**, 2957 (1994).
[37] B.D. Thoms and J.E. Butler, Surf. Sci. **328**, 291 (1995).
[38] Y. Kuang, N. Lee, A. Badzian, T.T. Tsong, T. Badzian, and C. Chen, Diamond Relat. Mater. **4**, 1371 (1995).
[39] Y. Kuang, Y. Wang, N. Lee, A. Badzian, T. Badzian, and T.T. Tsong, Appl. Phys. Lett. **67**, 3721 (1995).
[40] P.B. Lukins, M.H. Zareie, and J. Khachan, Appl. Phys. Lett. **78**, 1520 (2001).
[41] G. Kresse and J. Furthmüller, Phys. Rev. B **54**, 11 169 (1996).
[42] G. Kresse and J. Furthmüller, Comput. Mater. Sci. **6**, 15 (1996).
[43] P.E. Blöchl, Phys. Rev. B **50**, 17 953 (1994).
[44] G. Kresse and D. Joubert, Phys. Rev. B **59**, 1758 (1999).
[45] J.P. Perdew and A. Zunger, Phys. Rev. B **23**, 5048 (1981).
[46] D.M. Ceperley and B.J. Alder, Phys. Rev. Lett. **45**, 566 (1980).
[47] J.P. Perdew, J.A. Chevary, S.H. Vosko, K.A. Jackson, M.R. Pederson, D.J. Singh, and C. Fiolhais, Phys. Rev. B **46**, 6671 (1992).
[48] J. Furthmüller, J. Hafner, and G. Kresse, Phys. Rev. B **50**, 15 606 (1994).
[49] M. Schwoerer-Böhning, A.T. Macrander,and D. Arms, Phys. Rev. Lett. **80**, 5572 (1998).
[50] F. Favot and A. Dal Corso, Phys. Rev. B **60**, 11 427 (1999).
[51] P. Pulay, Chem. Phys. Lett. **73**, 393 (1980).
[52] J.E. Northrup, Phys. Rev. B **44**, 1419 (1991).
[53] B.D. Thoms and J.E. Butler, Phys. Rev. B **50**, 17 450 (1994).